Rev. Ivoir. Sci. Technol., 42 (2023) 190 - 198
ISSN 1813-3290, http://www.revist.ci

BRITTLE CRACKS IN A THREE-DIMENSIONAL ELASTIC HALF-SPACE UNDER THE RECTILINEAR CONTACT PRESSURE OF A CYLINDER : INTRODUCING GRAVITATIONAL FORCES

P. N. B. ANONGBA

Université F.H.B. de Cocody, U.F.R. Sciences des Structures de la Matière et de Technologie, 22 BP 582 Abidjan 22, Côte d'Ivoire

(reçu le 19 Novembre 2023; accepté le 22 Décembre 2023)

* Correspondance, e-mail : *anongba@gmail.com*

ABSTRACT

This study considers a three-dimensional brittle elastic half-space on the flat Ox_1x_3- plane boundary of which an infinitely long cylinder lies along the Ox_3-contact line and in presence of gravitational forces. Under the load P (per unit length) exerted by the cylinder along the x_2- direction, fracture propagates over large distance. The expected crack is planar with a straight front parallel to x_3, inclined with respect to x_1x_3 by an angle θ. The crack under load is represented by a continuous distribution of two straight edge dislocation families J (J= // and ⊥) parallel to x_3 with Burgers vectors $b_{//}$ and $b_{\perp}$ parallel and perpendicular to the solid flat surface. Analytical expressions for crack-tip stresses, crack extension force G (per unit length of the crack front), spatial forms about the crack tip of crack dislocation distributions D_J and corresponding relative displacement ϕ_J of the faces of the crack are obtained. These make it possible to account for the commonly observed fact that cracks can break into two pieces very large blocks of stone in absence of externally applied forces from the experimenter.

Keywords : *fracture mechanics, linear elasticity, dislocations, singular integral equations, Poisson effect.*

RÉSUMÉ

Fissures fragiles dans un demi-espace élastique à trois dimensions sous la pression de contact rectiligne d'un cylindre : présentation des forces gravifiques

Cette étude considère un demi-espace élastique fragile à trois dimensions avec comme surface le plan Ox_1x_3, sur lequel un cylindre infiniment long est couché, le long de la ligne de contact Ox_3 ; les forces gravifiques sont prises en compte. Sous la charge P (par unité de longueur) exercée par le cylindre dans la direction x_2, la rupture se propage sur une grande distance. La fissure attendue est plane avec un front droit parallèle à x_3, inclinée par rapport à x_1x_3 d'un angle θ. La fissure sous charge est représentée par une distribution continue de deux familles de dislocations droites J (J= // et $\perp$) parallèles à x_3 de vecteurs de Burgers $\vec{b}_{//}$ et $\vec{b}_{\perp}$ parallèles et perpendiculaires à la surface plane du solide. Des expressions analytiques pour les contraintes en tête de fissure, force d'extension de fissure G (par unité de longueur du front de fissure), dépendances spatiales au niveau du front de fissure des distributions de dislocation de fissure D_J et déplacement relatif correspondant ϕ_J des faces de la fissure sont obtenues. Celles-ci permettent de tenir compte du fait couramment observé selon lequel des fissures peuvent briser, en deux morceaux, de très gros blocs de pierre en l'absence de forces appliquées extérieurement par l'expérimentateur.

Mots-clés : *mécanique de la rupture, dislocation, équation intégrale singulière, effet poisson.*

I - INTRODUCTION

The present study aims at introducing gravitational forces in fracture mechanics. The motivation comes from the following common observation. Blocks of stone with large dimensions (say of the order of three meters or larger) can be easily fractured into two pieces ***(Figure 1)***. First, cylindrical holes are introduced at top surface using drills. Second, fracture is initiated from the holes with the help of sledgehammers and wedges. Without any additional action, the crack will move with time downward other very large distance and separate the block of stone into two parts. The fracture surface is perfectly flat. This sentence can be posed: a crack with a critical size in a solid can begin an expansion under gravitational forces only to split completely into two pieces a large solid. The explanation is as follows. The weight $\sigma_{22}^{AW} = \rho g x_2$ increases downward vertically (along the x_2-direction), with the position x_2 of the crack front (ρ is the density of the stone and g the acceleration due to gravity); in the

two other directions x_1 and x_3 exist induced normal Poisson's stresses $-\nu_A\sigma_{22}^{AW}$ (ν_A is Poisson's ratio). These are Poisson's stresses that produce induced macroscopic tensile forces perpendicular to the crack plane. These promote failure of the stone over large distance. To do so, we shall refer to the crack model used in a previous work [1] ***(Figure 2)***. This is a three-dimensional elastic half-space on the flat boundary of which is posed, in the x_3- direction, a long cylinder with radius R.

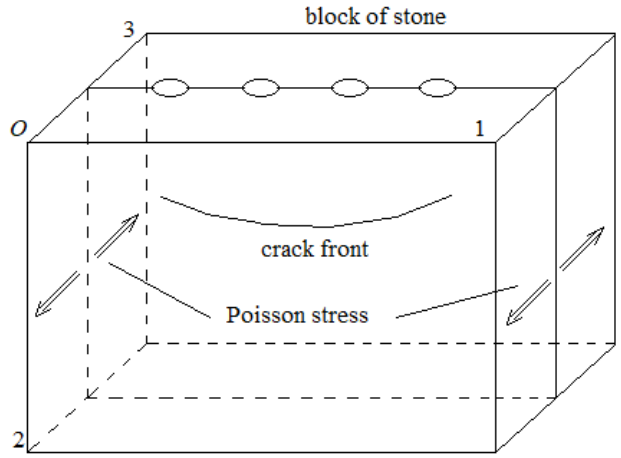

Figure 1 : *Block of stone with four holes at top surface to introduce fracture with the help of sledgehammer and wedge. The crack initiates and moves downward. These are Poisson's stresses which produce macroscopic tensile forces perpendicular to the crack plane; these induced tensile forces produce failure of the stone over large distance. The weight of the stone is the externally applied force and Poisson's forces are induced normal forces*

A planar straight-fronted crack with length $AB=l$, inclined around x_3 by angle θ from the surface, is present ; $OA = (a_1, a_2, 0)$ and $OB = (b_1, b_2, 0)$. This is an expected crack configuration at large distance from the cylinder under contact pressure; this is explained in [1]. The crack under load is represented by a continuous distribution of dislocations with infinitesimal Burgers vectors. The stress induced by the crack is equivalent to that produced by the dislocations. Two straight edge dislocation families J (J= // and $\perp$) parallel to x_3 with Burgers vectors $\vec{b}_{//} = (b,0,0)$ and $\vec{b}_{\perp} = (0,b,0)$ parallel and perpendicular to the solid flat surface are considered. To a crack dislocation J located at x_1 is associated an elevation h from Ox_1x_3 ***(Figure 2)*** with distribution function D_J such that $D_J(x_1^{'})dx_1^{'}$ represent the number of crack dislocations J in small x_1- interval $dx_1^{'}$ about $x_1^{'}$. It is required to find the equilibrium dislocation

distributions under the combined actions of the cylinder $(\sigma)^A$, gravitational forces $(\sigma)^{AW}$ and crack dislocation stresses $(\sigma)^{(J)}$. The methodology is given in *Section* 2, very similar to that described in [1] where $(\sigma)^A$ and $(\sigma)^{(J)}$ are given. Results are provided in *Section* 3. Discussion and conclusion form *Sections* 4 and 5.

II - METHODOLOGY

We consider one crack in the half-space, located between *A* and *B* in the Ox_1x_2-plane ***(Figure 2)*** as described in *Section* 1. The crack system is completely.

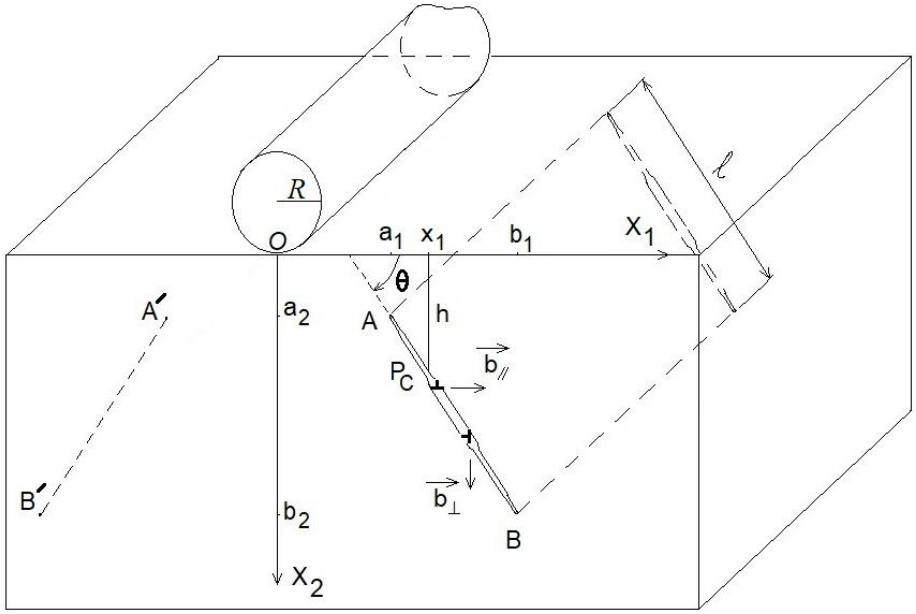

Figure 2 : *Brittle elastic half-space under load by a cylinder (P is the load per unit length of the cylinder) posed along the x_3- direction on its flat boundary surface; a planar crack of finite extension l is present, located between positions A and B in the Ox_1x_2 - plane and inclined by angle θ from the planar boundary. The crack front is straight, parallel to the cylinder axis. Our modelling assumes the half-space to be infinitely extended and the cylinder (radius R) and crack to run indefinitely along the x_3- direction*

defined when the dislocation distributions D_J (J= // and $\perp$) are known. For this purpose, we ask the crack faces to be free from traction:

$$\begin{cases} \bar{\sigma}_{12} - \partial h / \partial x_1 \bar{\sigma}_{11} = 0 \\ \bar{\sigma}_{22} - \partial h / \partial x_1 \bar{\sigma}_{12} = 0 \end{cases}. \tag{1}$$

$(\bar{\sigma})$ *is the stress at any position* $P(x_1, x_2, x_3)$ *in the medium and is linked to* D_J. *In (1), we are concerned with the point* $P_C(x_1, x_2 = h(x_1), x_3)$ *of the crack faces only.*

$$(\bar{\sigma}) = (\sigma)^A + (\sigma)^{AW} + (\bar{\sigma})^{(//)} + (\bar{\sigma})^{(\perp)} \tag{2}$$

$$\bar{\sigma}_{ij}^{(J)}(P) = \int_{a_1}^{b_1} \sigma_{ij}^{(J)}(x_1 - x_1', x_2, x_3) D_J(x_1') dx_1' \quad (J = // \text{ and } \perp). \tag{3}$$

$\sigma_{ij}^{(J)}$ is the stress produced by a dislocation *J* located at an elevation $h(x_1')$ from the half-space boundary. (1) provides two integral equations with Cauchy-type singular kernels that determine the D_J. When these have been found, the relative displacement ϕ_J of the faces of the crack, crack-tip stresses, and crack extension force *G* per unit length of the crack front are obtained by integrations (*Section* 3).

III - RESULTS

III-1. Crack dislocation distributions

We just need to use the spatial dependence of D_J about the crack tip *B*. The condition (1) can be managed to read:

$$\begin{cases} f_{//}^{A-W}(B) + C_1 \int_{1-\delta b_1/b_1}^{1} dy_1' D_{//}(y_1') \dfrac{1}{1-y_1'} = 0 \\ f_{\perp}^{A-W}(B) + C_1 \int_{1-\delta b_1/b_1}^{1} dy_1' D_{\perp}(y_1') \dfrac{1}{1-y_1'} = 0 \end{cases}; \tag{4}$$

$f_{//}^{A-W}(B) = \sigma_{12}^{A} + \sigma_{12}^{AW} - p_0(\sigma_{11}^{A} + \sigma_{11}^{AW})$, $f_{\perp}^{A-W}(B) = \sigma_{22}^{A} + \sigma_{22}^{AW} - p_0(\sigma_{12}^{A} + \sigma_{12}^{AW})$ $p_0 = \tan\theta$, $C_1 = \mu b / 2\pi(1-\nu)$. Here ν is Poisson's ratio and μ is the shear modulus. Inverting (4) in a similar way as in [2], we arrive at

$$D_J \cong \alpha_0 \alpha_J \frac{1}{\sqrt{1-y_1}}, \quad \phi_J \cong 2b\alpha_0 \alpha_J b_1 \sqrt{1-y_1}\ ; \tag{5}$$

$\alpha_J = f_J^{A-W} / \pi C_1$, $y_1 = x_1 / b_1$, $(1\text{-}y_1)$ positive infinitesimal value and α_0 dimensionless constant [2].

III-2. Crack-tip stresses

In the crack plane and ahead of the crack-tip at spatial position $P_C(x_1 = b_1 + s, x_2 = h(x_1), x_3)$, $0 < s << b_1$, the total stress $\bar{\sigma}_{ij}(P_C)$ is identified to the following formula.

$$\bar{\sigma}_{ij}(s) = \sum_{J=//\text{and}\perp} \int_{b_1-\delta b_1}^{b_1} \sigma_{ij}^{(J)}(b_1 + s - x_1^{'}) D_J(x_1^{'}) dx_1^{'}, \quad \delta b_1 << b_1. \tag{6}$$

This formula means that only those dislocations located about the crack front in x_1- interval $[b_1 - \delta b_1, b_1]$ will contribute significantly to the stress at $x_1 = b_1 + s$ ahead of the crack-tip as s tends to zero; any other contribution will become negligible for a sufficiently small value of s. Using (5) for D_J and integrating (6), we obtain

$$\bar{\sigma}_{12}(s) = \frac{(1-p_0^2)}{(1+p_0^2)^2}(\alpha_{//} + p_0\alpha_\perp) C_1\alpha_0 \frac{\pi\sqrt{b_1}}{2\sqrt{s}},$$

$$\bar{\sigma}_{11}(s) = \frac{1}{(1+p_0^2)^2}\left[(1-p_0^2)\alpha_\perp - p_0(3+p_0^2)\alpha_{//}\right] C_1\alpha_0 \frac{\pi\sqrt{b_1}}{2\sqrt{s}},$$

$$\bar{\sigma}_{22}(s) = \frac{1}{(1+p_0^2)^2}\left[p_0(1-p_0^2)\alpha_{//} + (1+3p_0^2)\alpha_\perp\right] C_1\alpha_0 \frac{\pi\sqrt{b_1}}{2\sqrt{s}},$$

$$\bar{\sigma}_{33}(s) = \frac{2\nu}{1+p_0^2}(\alpha_\perp - p_0\alpha_{//}) C_1\alpha_0 \frac{\pi\sqrt{b_1}}{2\sqrt{s}},$$

$$\bar{\sigma}_{j3} = 0, \quad j = 1 \text{ and } 2. \tag{7}$$

III-3. Crack extension force

Our expression of the crack extension force is taken from [3] and used extensively (see [4 - 7], for example). It can be checked, easily, that this also applies in presence of gravitational forces. A crack of length l is considered at equilibrium under load (use ***Figure 2*** for illustration). Then, this crack grows almost statically over a short distance from one of its ends (say $x_1 = b_1$) while the other end remains fixed. A work associated with a newly created surface element Δs is then calculated, which is the product of the elastic force (using (7)) on the element (just before the motion of the crack tip) by the relative displacement of the faces of the newly created crack through Δs (using (5)). This energy is then divided by Δs ; the limit G taken by the ratio of that energy divided by Δs when the latter tends to zero is by definition the crack extension

force per unit length of the crack front at the point P_C where Δs is located. We obtain at B (b_1, $h(b_1)$, x_3)

$$G(B) = \frac{2(1-\nu)b_1\alpha_0^2}{\mu\sqrt{1+p_0^2}}\left(\left[f_{//}^{A-W}(B)\right]^2 + \left[f_{\perp}^{A-W}(B)\right]^2\right). \quad (8)$$

For numerical application, we take A to coincide with the origin O ***(Figure 2)*** and both the medium and cylinder to have equal density ρ. We define $\tilde{G}$ a reduced value of G as

$$\tilde{G} = \frac{G(B)}{G_0}, \quad G_0 = 2(1-\nu)(\alpha_0\rho g)^2 R^3/\mu \ . \quad (9)$$

When applied to the solid posed on the surface of earth, the specimen suffers compression, so we write $\sigma_{22}^{AW} = -\rho g x_2$. $\tilde{G}$ is written as a function of $\tilde{b}_2 = b_2/R$ for three different values of θ in ***Figure 3*** and as a function of θ for three values of $\tilde{b}_2$ in ***Figure 4***.

IV - DISCUSSION

The modelling is considered applicable for large cracks with B far from the cylinder. To estimate the appropriate height $\tilde{b}_2(B_C)$ of B at which gravitational forces only will break into two pieces the medium, from ***Figure 3***, this would occur at $B = B_C$ for which $G(B_c) = 2\gamma$ in steady motion, where γ is the surface energy. α_0 may be provided from experiment as an adjustable parameter.

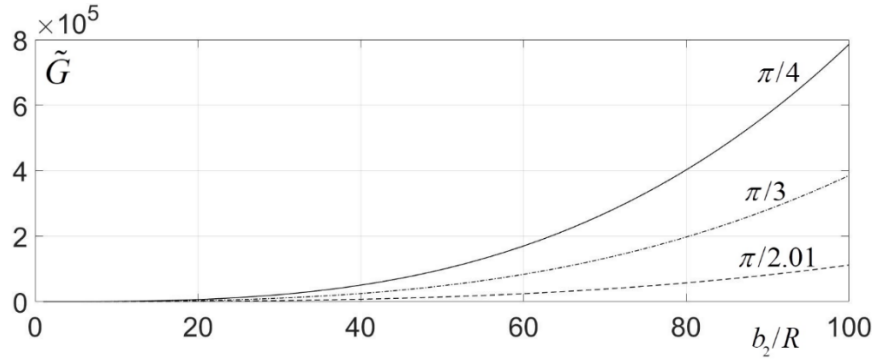

Figure 3 : *$\tilde{G}$ (9) as a function of $\tilde{b}_2 = b_2/R$ for three different values of θ. It increases continuously with $\tilde{b}_2$*

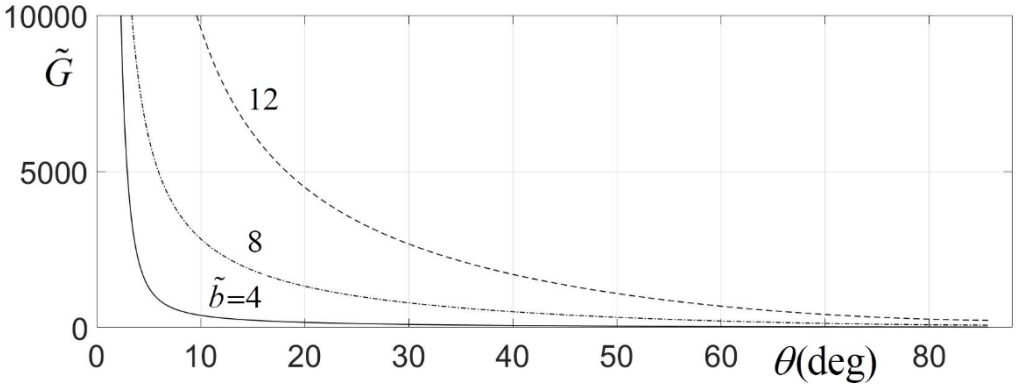

Figure 4 : *$\tilde{G}$ (9) as a function of θ for three different values of $\tilde{b}_2$. It decreases continuously with θ*

Figure 1 corresponds to $\theta = \pi/2$ with the cylinder *(see **Figure 2**)* on the four holes of the top surface. From ***Figure 4***, it is seen that $\tilde{G}$ is larger for small θ in agreement with observations; we can refer to [8] : ***Figure 5*** is reproduced from his Fig. 8.3, page 254. The depth of the crack or equivalently the length of the crack can be evaluated in steady motion as follows. For smaller θ values *(use **Figure 4**)*, G is larger than 2γ for the crack is observed; then it decreases with depth and should stop inside the medium when $G \leq 2\gamma$. Because of the small size of the specimen in ***Figure 5***, gravitational forces are probably negligeable. Under gravitational forces, solids suffer compression. Hence, fracture surfaces over large distance will be aligned parallel to ***g***, the acceleration due to gravity, that becomes a zone axis for families of fracture planes.

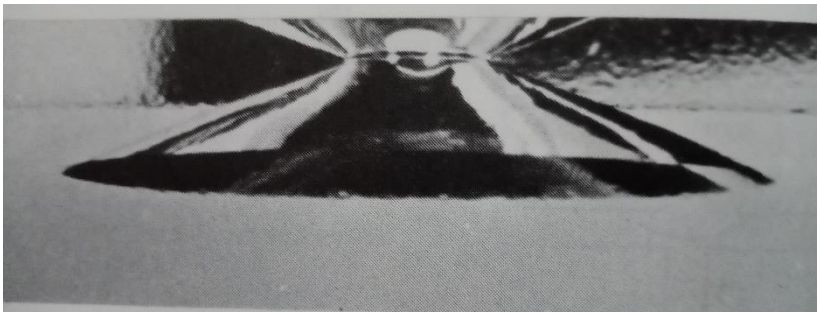

Figure 5 : *Cone crack in soda-lime photographed under load (P = 40kN) from cylindrical punch, optical microscopy. The present block edge is 38.7 mm length approximately. Crack makes angle 22° to free surface. (After Roesler, F.C. (1956) Proc. Phys. Soc. Lond. B69 981)*

V - CONCLUSION

In conclusion, we have investigated fracture propagation in a three-dimensional elastic half-space subjected to the rectilinear contact pressure of a cylinder lying on the flat Ox_1x_3- plane boundary and in presence of gravitational forces. Analytical expressions have been obtained for G, the crack extension force per unit length of the crack front. That is a merit of the work. This makes it possible to account for the commonly observed fact that cracks can break into two pieces very large blocks of stone in absence of externally applied forces from the experimenter.

REFERENCES

[1] - P. N. B. ANONGBA, *Rev. Ivoir. Sci. Technol.*, 34 (2019) 25 - 43
[2] - P. N. B. ANONGBA, *Rev. Ivoir. Sci. Technol.*, 38 (2021) 388 - 409
[3] - B. A. BILBY and J. D. ESHELBY, In:" Fracture", Ed. *Academic Press (H. Liebowitz), New York,* Vol. 1, (1968) 99 - 182
[4] - P. N. B. ANONGBA, *Rev. Ivoir. Sci. Technol.*, 16 (2010) 11 - 50
[5] - P. N. B. ANONGBA, J. BONNEVILLE and A. JOULAIN, *Rev. Ivoir. Sci. Technol.*, 17 (2011) 37 - 53
[6] - P. N. B. ANONGBA, *Rev. Ivoir. Sci. Technol.*, 26 (2015) 76 - 90
[7] - P. N. B. ANONGBA, *Rev. Ivoir. Sci. Technol.*, 32 (2018) 10 - 47
[8] - B. R. LAWN, "Fracture of Brittle Solids – Second Edition", Cambridge University Press, Cambridge, (1993)